Effect of Phonon Scattering by Surface Roughness on the Universal Thermal Conductance

D. H. Santamore and M. C. Cross

Department of Physics, California Institute of Technology 114-36, Pasadena, California 91125

(Received 21 May 2001; published 24 August 2001)

The effect of phonon scattering by surface roughness on the thermal conductance in mesoscopic systems at low temperatures is calculated using full elasticity theory. The low frequency behavior of the scattering shows novel power law dependences arising from the unusual properties of the elastic modes. This leads to new predictions for the low temperature depression of the thermal conductance below the ideal universal value. Comparison with the data of Schwab *et al.* [Nature (London) **404**, 974 (2000)] suggests that surface roughness on a scale of the width of the thermal pathway is important in the experiment.

DOI: 10.1103/PhysRevLett.87.115502 PACS numbers: 63.22.+m, 63.50.+x, 68.65.–k

Thermal transport in mesoscopic systems at low temperatures shows universal properties analogous to the quantized electrical conductance [1]. Theoretical analyses of phonon transport when the thermal wavelength becomes comparable to the dimensions of the thermal pathway predict a thermal conductance K that is independent of many of the details of the geometry and material properties [2], and a universal value for $K/T = N_0\pi^2 k_B^2/3h$ at low enough temperatures [3,4]. (Here N_0 is the number of modes with zero frequency at long wavelengths, equal to 4 for a single, free-standing elastic beam.) These predictions have since been connected to more general results on bounds on entropy transport at low temperatures [5] and to thermal transport by particles of arbitrary statistics [6]. The recent confirmation of the universal thermal conductance in tiny silicon nitride devices [7] is an experimental tour de force. Although verifying the predictions of a universal value of K/T at low enough temperatures, the experiments showed values of K/T that *decrease* as the temperature increases in the range of 0.08 to 0.2 K, before beginning to rise at higher temperatures as more vibrational modes that can carry the heat are excited.

We [8] and others [9,10] have previously studied a simplified treatment of this problem using a scalar model for the elastic waves. However, elastic waves in confined geometries have many unusual features, such as modes with a quadratic dispersion relation $\omega \propto k^2$ at small wave numbers k and regions of anomalous dispersion $d\omega/dk < 0$, that are not captured in this simple model and might be expected to have a strong influence on the low temperature transport.

In this Letter we study the general problem of the scattering of phonons by rough surfaces for a rectangular cross-section elastic beam using three-dimensional elasticity theory. The scattering of the low frequency modes that contribute to the conductance at low temperatures depends on the detailed properties of the elastic modes, and we find novel power law dependences for the frequency dependence of the scattering off unstructured roughness that are *not* those anticipated by simple analogy with Rayleigh scattering. In turn this low frequency behavior yields a depression of K/T at low temperatures with unexpected power laws, with a faster decrease of K/T as the temperature is raised than anticipated from the scalar model. Comparing these predictions with the experiments of Schwab *et al.* [7] suggests that unstructured roughness is inadequate to explain the data: instead we find that a roughness length scale comparable to the width yields a fit consistent with the experimental trends.

In the ballistic transport regime, the thermal conductance at temperature T takes the form [2–4]

$$K = \frac{\hbar^2}{k_B T^2} \sum_m \frac{1}{2\pi} \int_{\omega_m}^{\infty} T_m(\omega) \frac{\omega^2 e^{\beta\hbar\omega}}{(e^{\beta\hbar\omega} - 1)^2} \, d\omega \,, \quad (1)$$

where the sum is over the modes m propagating in the structure, ω_m is the cutoff frequency of the mth mode, and $\beta = 1/(k_B T)$. The parameter $T_m(\omega)$ is the transmission coefficient: $T_m(\omega) \neq 1$ corresponds to a reduction in the transport due to some scattering process. At low temperatures, only the modes with $\omega_m = 0$ contribute, and in the absence of scattering the conductance takes on its universal value K_u.

To calculate the transmission coefficient $T_m(\omega)$ in Eq. (1) we use a Green function method similar to the one previously reported in the scalar-wave calculation [8]. The thermal pathway is modeled as a rectangular elastic beam or waveguide of width W, depth d, and length L in the x-direction. We assume smooth top and bottom surfaces corresponding to the epitaxial growth planes, and rough surfaces at $y = \pm W/2 + f_{\pm}(x)$ deriving from the lithographic processing. The functions $f_{\pm}(x)$ define the roughness, which we assume to be independent of the z coordinate and small $f_{\pm} \ll W$.

Assuming isotropic elasticity theory, the displacement field $\mathbf{u}$ satisfies the wave equation,

$$\rho \, \partial^2 u_i/\partial t^2 - \partial T_{ij}/\partial x_j = 0 \,, \quad (2)$$

where ρ is the mass density, and T_{ij} is the stress tensor, $T_{ij} = C_{ijkl}\partial_k u_l$, with C_{ijkl} the elastic modulus tensor.

Stress-free conditions apply at the surfaces $T_{ij}n_j|_S = 0$ with $\mathbf{n}$ being the surface normal. The Green function $G_{ij}(\vec{x}, \vec{x}'; t)$ is defined to satisfy the corresponding equation with a source term $\delta_{ij}\delta(\mathbf{x} - \mathbf{x}')\delta(t - t')$, on the right-hand side, and stress-free boundary conditions at the smoothed surfaces $y = \pm W/2$. Using the completeness of the orthonormal, smooth-surface, elastic modes $\mathbf{u}_k^{(n)}(\mathbf{x}, \omega)$ at frequency ω (with k the wave number along the waveguide and n labeling the transverse mode structure), the Fourier transformed Green function can be written in the form

$$G_{ij}(\vec{x}, \vec{x}'; \omega) = i \sum_n \frac{u_i^{(n)*}(\vec{x}', \omega) u_j^{(n)}(\vec{x}, \omega)}{2\rho\omega v_g^{(n)}}, \qquad (3)$$

The sum is over the elastic modes n that propagate at frequency ω: the condition $\omega(k) = \omega$, with $\omega(k)$ the dispersion relation, defines a discrete set of wave numbers k_n and corresponding mode indices n. For monotonic $\omega(k)$ there is a single solution for k on each branch [defined by a continuous $\omega(k)$], but with anomalous dispersion there may be multiple solutions. $v_g^{(n)}$ is the group velocity of mode n at frequency ω.

The stress-free boundary conditions for the propagating waves apply at the actual (rough) surfaces; expanding in small $f_\pm$ leads to effective stress boundary conditions at the smooth surfaces $y = \pm W/2$, which can then be included using Green's theorem. These manipulations lead to the expression for the scattered field $\mathbf{u}^{(sc)}$ to lowest order in the small roughness in terms of the stress field of the incident wave at $y = \pm W/2$. The backscattered field from a unit-amplitude incident wave in mode m is

$$\vec{u}^{(sc)} = \sum_{n, v_g^{(n)} < 0} \frac{i\vec{u}^{(n)}(\vec{x}, \omega)}{2\rho\omega v_g^{(n)}} \int_{-\infty}^{\infty} f_\pm(x') \Gamma_\pm^{(m,n)}(x', \omega)\, dx', \qquad (4)$$

with

$$\Gamma_\pm^{(m,n)} = \int dz \{\rho\omega^2 u_i^{(m)} u_i^{(n)*} - E^{-1}[(T_{xx}^{(m)} T_{xx}^{(n)*} + T_{zz}^{(m)} T_{zz}^{(n)*}) - \sigma(T_{xx}^{(m)} T_{zz}^{(n)*} + T_{zz}^{(m)} T_{xx}^{(n)*})] + \mu^{-1} T_{zx}^{(m)} T_{xz}^{(n)*}\}_{y=\pm W/2} \qquad (5)$$

(repeated indices i and $\pm$ are to be summed over), where E is Young's modulus, $\mu = E/2(1 + \sigma)$ is the shear modulus, σ is the Poisson ratio, and $T_{ij}^{(n)}$ is the stress field corresponding to the displacement field $\mathbf{u}^{(n)}$. The mode sum in Eq. (4) is confined to modes propagating to *negative x*, i.e., $v_g^{(n)}(k_n) < 0$: usually these will be modes with negative wave numbers k_n, but there are also regions of anomalous dispersion which have a negative group velocity for positive k_n. Notice that Eq. (4) is comprised of separate kinetic, compression, and shear terms.

We now study the *thin plate limit* $d \ll W$ [11,12], which yields closed form expressions for the displacement fields of the modes (in terms of a dispersion curve $\omega(k)$ given by a numerical solution of a simple transcendental equation). This approach correctly accounts for the important properties of the elastic modes, for example, exactly reproducing the small k dispersion relations, including the quadratic dispersion of the bend modes, and showing regions of anomalous dispersion, while at the same time allowing analytic progress.

Thin plate theory should be quantitatively accurate for many mesoscopic experiments where the thickness of the sample (formed by epitaxial growth) is often much less than the width (given by lithography). The dispersion curves in the thin plate approximation are shown in Fig. 1. Note that the modes polarized in the plane and perpendicular to the plane (flexural modes) do not couple.

An important simplification in thin plate theory is that all z components of the stress tensor T_{iz}, T_{zi} in Eq. (5) may be put to zero [11]. The expression for the flux scattering rate (per unit length of rough waveguide) from mode m to mode n at frequency ω, defined as $|v_g^{(n)}/v_g^{(m)}|$ times the ratio of the mode intensities, simplifies to

$$\gamma_{m,n}(\omega) = \frac{\omega^2 \tilde{g}(k_m - k_n)}{2|v_g^{(m)} v_g^{(n)}| W^2} \left| \int dz \left\{ \phi_i^{(m)} \phi_i^{(n)*} - \frac{E k_m k_n}{\rho\omega^2} \phi_x^{(m)} \phi_x^{(n)*} \right\}_{y=W/2} \right|^2, \qquad (6)$$

where ϕ gives the transverse dependence of the modes $u_i^{(n)} = e^{ik_n x} \phi_i^{(n)}(y, z)$. To arrive at this expression we performed an ensemble average over the surface roughness function $f_\pm(x)$, and $\tilde{g}(k)$ is the spectral density, i.e., the Fourier transform of the roughness correlation function $g(x)$ defined by

$$\langle f(x) f(x') \rangle = g(x - x'), \qquad (7)$$

where f is f_+ or f_-, and we assume independent scattering off the two rough surfaces introducing a factor of 2 into Eq. (6). For weak scattering the transmission coefficient appearing in the equation for the thermal conductance Eq. (1) can be obtained as $T_m = e^{-\gamma_m L}$ with $\gamma_m = \sum_{n, v_g^{(n)} < 0} \gamma_{m,n}$, where we sum only over the backscattering, since scattering into forward propagating modes does change the heat transport.

We first study the scattering behavior for unstructured "white noise" roughness, $\tilde{g}(k) = \tilde{g}(0)$ independent of k. At low frequencies only the four lowest modes with zero onset frequency survive (the compression mode and a

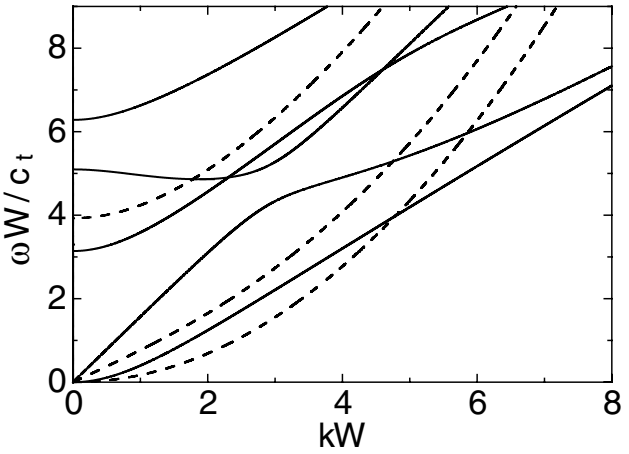

FIG. 1. Dispersion relation for in-plane modes (solid lines) and flexural modes (dashed lines) for a geometry ratio $d/W = 0.375$ and Poisson ratio 0.24. The wave numbers are scaled with the width W and the frequencies by W/c_t with $c_t = \sqrt{\mu/\rho}$.

bending mode polarized in the plane, and the torsion mode and a second bending mode polarized perpendicular to the plane). Explicit expressions for the scattering coefficients from these modes, $\gamma_m(\omega)W^4/\tilde{g}(0)$, are shown in Table I as a function of the scaled frequency $\bar{\omega} = \omega c_E/W$ with $c_E = \sqrt{E/\rho}$ the propagation speed of extension waves in the beam. Notice that the backscattering from the compression mode to the time reversed mode, and from the torsion mode to its time reversed mode, has the ω^2 dependence anticipated in analogy with $1d$ Rayleigh scattering (as indeed was found in the scalar-wave calculation). On the other hand, scattering to or from the bending modes introduces quite different power law dependences that will dominate at low frequencies. Most of this novel behavior can be understood simply from the prefactor in Eq. (6), $\gamma \propto \omega^2/v_g^{(m)}v_g^{(n)}$, since v_g goes to a constant at small frequencies for the compression and torsion modes, and is proportional to $\omega^{1/2}$ for the bending modes. The remaining part of Eq. (6), the integral over z, is $O(1)$ as $\omega \to 0$, except for the flexural bending mode backscattering where the kinetic and stress contributions cancel at leading order. Note also that the expressions for the flexural modes involve additional factors of the width-to-depth ratio W/d, so that in the thin plate limit these modes will be scattered more strongly at a given ω.

The low temperature thermal conductance can be derived directly from the low frequency scattering expressions: if we write these as $\gamma L = A\bar{\omega}^p$, then the corresponding contribution of the suppression of the thermal conductance is

$$\delta K/K_u = AI_p(T/T_E)^p \tag{8}$$

where $T_E = \hbar c_E/k_B W$, and I_p is the integral

$$I_p = \frac{3}{\pi^2}\int_0^\infty dy\, \frac{y^{p+2}e^y}{(e^y - 1)^2}, \tag{9}$$

giving the same power law for the temperature dependence.

Figure 2 shows the scattering coefficients over an extended frequency range, again with $\tilde{g}(k) = \text{const}$. The phonons are strongly scattered at each mode onset frequency, as a result of the zero group velocity and the correspondingly large density of states to scatter into. We find additional strong scattering in the regions of anomalous dispersion (e.g., $\omega W/c_t \simeq 5$), since again these portions of the dispersion curve are quite flat. Also, since the group velocity of the in-plane bending mode approaches zero, the scattering of this mode increases relative to others as $\omega \to 0$. This agrees with the low frequency analysis, $\gamma \propto \omega$. For intermediate frequencies $0.08 < \omega W/c_t < 1.8$ the scattering of the torsion mode is larger than for the other modes.

With this detailed understanding, we now attempt to fit the experiments of Schwab *et al.* We focus on the data below 0.4 K, where thin plate theory captures the relevant modes [13]. To compare with experiment we first subtract the *measured* conductance from the ideal conductance predicted using the cutoff frequencies *calculated* numerically by using the *xyz* approach [14] and $d = 60$ nm and $W = 160$ nm: this gives us an estimate of the effect of scattering which we can compare with our calculated scattering. The data processed in this way (Fig. 3) show an abrupt onset of scattering at some nonzero temperature ($T \sim 0.08$ K): this does not appear to be consistent with the power law behavior predicted using unstructured roughness [Table I and Eq. (8)]. Notice that the discrepancy is worse than anticipated in the scalar-wave calculation [8], which gave larger exponents for the power law dependence. The delay in the onset of scattering suggests that the phonons with long wavelength are not much affected by the rough surfaces. To accommodate this fact,

TABLE I. Scattering coefficients for the zero onset frequency modes at low frequencies: c denotes compression, b denotes bend, t denotes torsion, bb denotes bend-to-bend scattering, etc. Values are quoted for $\gamma_m W^4/\tilde{g}(0)$ as a function of scaled frequency $\bar{\omega} = \omega c_E/W$. For the flexural bend-to-bend scattering (bb) the terms in the braces in Eq. (6) cancel to leading order, resulting in very small $O(\bar{\omega}^3)$ scattering. There is no scattering between in-plane and flexural modes for the z-independent roughness assumed.

In-plane			Flexural		
cc	*bb*	*bc*,*cb*	*tt*	*bb*	*tb*,*bt*
$2\bar{\omega}^2$	$\sqrt{3}\,\omega$	$\frac{3^{5/4}}{2^{3/2}}\bar{\omega}^{3/2}$	$\frac{9(1+\sigma)}{4}(\frac{W\bar{\omega}}{d})^2$	$O[(\frac{W\bar{\omega}}{d})^3]$	$\frac{3^{5/4}(1+\sigma)^{1/2}}{4}(\frac{W\bar{\omega}}{d})^{3/2}$

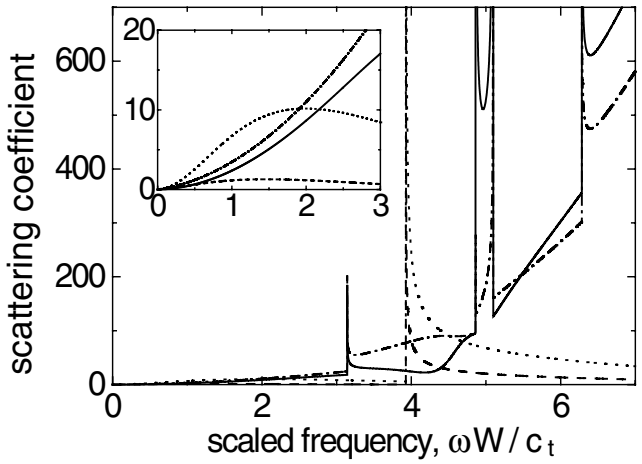

FIG. 2. Scattering coefficient $\gamma_m W^4/\tilde{g}(0)$ of the lowest (zero onset frequency) modes to all other modes for unstructured roughness; dash-dotted line: compression; solid line: in-plane bend; dashed line: flexural bend; dotted line: torsion. The inset shows the magnified view at low frequency with the same quantities plotted.

we have investigated the scattering by roughness centered around a finite length scale k_0^{-1}, using the parametrization

$$\tilde{g}(k) = \sqrt{\pi}\,\delta^2 a e^{-a^2(k-k_0)^2}. \tag{10}$$

For $k_0 a \gtrsim 1$ this results in strongly reduced scattering at long wavelengths. There are three roughness parameters that now characterize the surfaces: the roughness amplitude δ, the correlation length a, and shift k_0. We obtain a reasonable fit to the low temperature onset of the scattering using parameters $a/W = 3$, $\delta/W = 0.11$, and $k_0 W = 4.7$. These parameters correspond to significant roughness at length scales comparable to the width of the device, which appears consistent with the electron micrograph of the structure used [15].

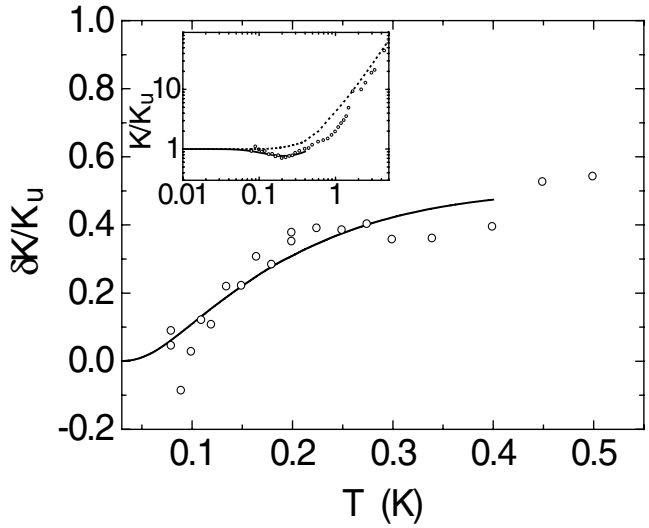

FIG. 3. Thermal conductance reduction relative to the universal value K_u as a function of temperature. Circles: data of Schwab *et al.* subtracted from the predicted ideal conductance; solid line: predictions from the elasticity calculation. The inset shows the thermal conductance relative to the universal value K_u as a function of temperature. Circles: data of Schwab *et al.*; dotted line: ideal conductance calculated using the *xyz* method; solid line: fit from elasticity theory with scattering. The roughness parameters used were $a/W = 3$, $\delta/W = 0.11$, and $k_0 W = 4.7$.

In summary, we have examined the scattering of phonons by surface roughness and the effect on the universal thermal conductance. At low temperature, the scattering shows strong dependence on the mode structure. In this temperature range, the elasticity model provides a better understanding of the scattering behavior and a reasonable fit to the experimental data, if we assume that the roughness is concentrated at a length scale comparable to the lithographic scale. Further experiments at lower temperatures would provide a useful test of the predictions of the theory.

This work was supported by NSF Grant No. DMR-9873573.

[1] R. Landauer, IBM J. Res. Dev. **1**, 223 (1957).
[2] D. E. Angelescu, M. C. Cross, and M. L. Roukes, Superlattices Microstruct. **23**, 673 (1998).
[3] L. G. C. Rego and G. Kirczenow, Phys. Rev. Lett. **81**, 232 (1998).
[4] M. P. Blencowe, Phys. Rev. B **59**, 4992 (1999).
[5] J. B. Pendry, J. Phys. A **16**, 2161 (1983).
[6] L. G. C. Rego and G. Kirczenow, Phys. Rev. B **59**, 13 080 (1999).
[7] K. Schwab, E. A. Henriksen, J. M. Worlock, and M. L. Roukes, Nature (London) **404**, 974 (2000).
[8] D. H. Santamore and M. C. Cross, Phys. Rev. B **63**, 184306 (2001).
[9] J. A. Sanchez-Gil, V. Freilikher, I. Yurkevich, and A. A. Maradudin, Phys. Rev. Lett. **80**, 948 (1998).
[10] A. Kambili, G. Fagas, V. I. Fal'ko, and C. J. Lambert, Phys. Rev. B **60**, 15 593 (1999).
[11] L. D. Landau and E. M. Lifshitz, *Theory of Elasticity* (Butterworth-Heinemann, Oxford, 1986).
[12] M. C. Cross and R. Lifshitz, Phys. Rev. B **64**, 085324 (2001).
[13] We compare the $k \to 0$ cutoff frequencies (which determine the ideal thermal conductance) obtained from thin plate theory with those from numerical solutions of the full $3d$ elasticity equations using the *xyz* algorithm [14] for the thickness-to-width ratio $d/W \simeq 0.4$ appropriate to the experimental geometry. For dimensionless frequencies $\omega W/c_t < 8$ (with c_t the propagation speed of transverse waves), thin plate theory gives a good approximation. Correspondingly, thin plate theory provides better than 5% accuracy for the ideal thermal conductance up to 0.4 K. The range of applicable temperature will improve with decreasing d/W.
[14] N. Nishiguchi, Y. Ando, and M. N. Wybourne, J. Phys. Condens. Matter **9**, 5751 (1997).
[15] K. Schwab (private communication).